Journal of Mining Science, Vol. 46, No. 6, 2010

ROCK FAILURE

WAVE PROPAGATION IN THE 2D PERIODICAL MODEL OF A BLOCK-STRUCTURED MEDIUM. PART I: CHARACTERISTICS OF WAVES UNDER IMPULSIVE IMPACT

N. I. Aleksandrova and E. N. Sher UDC 539.375

The authors use a two-dimension plane model to analyze seismic wave propagation in block-structured media under impulse loading. Dynamics of the medium is described by means of pendulum approximation, where blocks are considered incompressible and deformation and displacement occur via compressible intermediate layers. The simplest calculation model of a square lattice composed of masses and springs connected in axial and diagonal directions is under discussion in the article.

Block-structured medium, seismic waves, two-dimension lattice of masses, impulse loading, point source

Recent researches of seismic wave propagation in rocks have proved the need of making allowance for block-like structure of rocks in geomechanical and seismic math modeling. The fundamental conception of geomedium and its elements being structured as hierarchies of blocks was formulated by Sadovsky [1]: a rock mass is a system of various scale blocks that are nested in one another and mutually linked by intermediate layers composed of weaker and fractured rocks, this hierarchical system deforms nonlinearly and possesses complex rheology. Presence of pliant intermediate layers conditions that a block rock mass deforms due to deformation of these interbeds, both is statics and dynamics. It was said in [2 – 6] that a blocks structure together with its hierarchical pattern is a source of dynamic events that are absent in a homogeneous medium and, thus, beyond description with the homogeneous medium models. Such dynamic events are, for instance, pendulum waves. In terms of a homogeneous model, pendulum waves possess inexplicable properties: they are relatively long although generated by short impulsive input, and have low velocity. A number of studies into characteristics of pendulum waves with the use of one-dimension block models [7 – 11] showed that in a block-structured medium under impulsive exposure, the induced broadband perturbation, while propagating, falls into: high frequency waves incidental to natural vibration of the blocks, and low frequency waves. And it was revealed experimentally that high frequency waves attenuate fast, meanwhile the low frequency waves exercise major seismic effect. By calculations of undulatory motion in a chain of elastic rods with pliant inserts, the low frequency waves caused by impulsive impact are well described in a model of stiff blocks – visco-elastic interbeds. This approach to description of the dynamic behavior of a two-dimension medium composed of rigid rectangular blocks was used in [12 – 14]. A simplified model of a block-structured medium is possible with considering blocks the point masses connected by means of springs. Though evidently limited in capacity to describe real structures, periodic lattices are advantageous

Institute of Mining, Siberian Branch, Russian Academy of Sciences, E-mail: ensher@sibmail.ru, Novosibirsk, Russia. Translated from Fiziko-Tekhnicheskie Problemy Razrabotki Poleznykh Iskopaemykh, No. 6, pp. 57-68, November-December, 2010. Original article submitted October 14, 2010.

1062-7391/10/4606-0639 ©2010 Springer Science + Business Media, Inc.

for being able to build hierarchical models, to apply analytical and numerical calculation methods, qualitatively describe dynamic events in these structures and, not least, to get visual results. Theory of waves in periodic lattice structures, ensued from the classical study by Rayleigh [15] and founded on later scientific efforts [16 – 19], first found wide application in mechanics of composite structures and composite materials and was not used to characterize the rock mass hierarchy dynamics. Meanwhile, these researches and their outcomes are applicable in terms of seismology, e.g., in [20] the analysis of vibrations of lattices in antiplane statement discovered "star waves" that are the dynamic perturbation which propagates along rays governed by geometry of lattices. The analysis [21] of waves in a square lattice of masses under impulse impact was carried out in the antiplane statement. The two-dimension plane problem in [22] considered wave propagation in one-dimension and two-dimension structures "chains – masses" that were periodically loaded. The wave amplitude-frequency characteristics were examined, as well as the influence of bounds, viscosity and changed parameters of the structure on wave propagation behavior was shown.

This article is devoted to impulse-induced perturbations in a homogeneous two-dimension lattice composed of masses connected by springs in the directions of axes x, y and diagonally (Fig. 1). The problem is plane as in [22].

The motion equations of masses:

$$\begin{aligned} M\ddot{u}_{n,m} &= F^2 - F^6 + (F^1 + F^5 + F^3 + F^7)/\sqrt{2} + Q_x, \\ M\ddot{v}_{n,m} &= F^8 - F^4 + (F^1 + F^5 - F^3 - F^7)/\sqrt{2} + Q_y. \end{aligned} \tag{1}$$

Here, u and v are displacements in x and y directions, respectively; n and m are numbers of masses in x and y directions, respectively; M is mass; Q_x and Q_y are external forces. Forces F^i $(i = 1,...,8)$ are proportional to elongations of the related springs:

$$\begin{aligned} F^2 &= k_1(u_{n+1,m} - u_{n,m}), \quad F^6 = k_1(u_{n,m} - u_{n-1,m}), \\ F^8 &= k_1(v_{n,m+1} - v_{n,m}), \quad F^4 = k_1(v_{n,m} - v_{n,m-1}), \\ F^1 &= k_2(u_{n+1,m+1} - u_{n,m} + v_{n+1,m+1} - v_{n,m})/\sqrt{2}, \\ F^5 &= k_2(u_{n-1,m-1} - u_{n,m} + v_{n-1,m-1} - v_{n,m})/\sqrt{2}, \\ F^3 &= k_2(u_{n+1,m-1} - u_{n,m} + v_{n,m} - v_{n+1,m-1})/\sqrt{2}, \\ F^7 &= k_2(u_{n-1,m+1} - u_{n,m} + v_{n,m} - v_{n-1,m+1})/\sqrt{2}. \end{aligned} \tag{2}$$

Here, k_1 is spring stiffness in x and y directions; k_2 is diagonal spring stiffness.

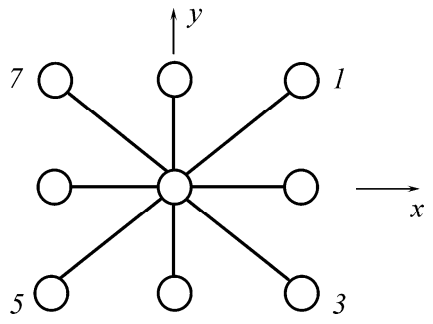

Fig. 1. Square lattice of masses and springs

Placing (2) in (1) transforms the motion equations into:

$$\begin{aligned} M\ddot{u}_{n,m} &= k_1(u_{n+1,m} - 2u_{n,m} + u_{n-1,m}) + k_2(u_{n+1,m+1} + u_{n-1,m-1} + u_{n+1,m-1} + \\ &+ u_{n-1,m+1} - 4u_{n,m})/2 + k_2(v_{n+1,m+1} + v_{n-1,m-1} - v_{n-1,m+1} - v_{n+1,m-1})/2 + Q_x, \\ M\ddot{v}_{n,m} &= k_1(v_{n,m+1} - 2v_{n,m} + v_{n,m-1}) + k_2(u_{n+1,m+1} + u_{n-1,m-1} - u_{n+1,m-1} - \\ &+ u_{n-1,m+1})/2 + k_2(v_{n+1,m+1} + v_{n-1,m-1} + v_{n-1,m+1} + v_{n+1,m-1} - 4v_{n,m})/2 + Q_y. \end{aligned} \tag{3}$$

We take the Laplace transform of time and Fourier transform of coordinates x, y and derive the following solution:

$$\hat{u} = \frac{(Mp^2 + a_{22})\hat{Q}_x - a_{12}\hat{Q}_y}{D(p, q_x, q_y)}, \quad \hat{v} = \frac{(Mp^2 + a_{11})\hat{Q}_y - a_{21}\hat{Q}_x}{D(p, q_x, q_y)},$$

$$D(p, q_x, q_y) = M^2 p^4 + Mp^2(a_{11} + a_{22}) + a_{11}a_{22} - a_{21}a_{12},$$

$$a_{11} = 2k_1[1 - \cos q_x l] + a, \quad a_{22} = 2k_1[1 - \cos q_y l] + a,$$

$$a = 2k_2[1 - \cos q_x l \cos q_y l], \quad a_{12} = a_{21} = 2k_2 \sin q_x l \sin q_y l.$$

In these equations: $\widehat{f}(p, q_x, q_y) = f^{LF_xF_y}$, L is the Laplace transform of time with parameter p; F_x, F_y are the discrete Fourier transforms of x and y with parameters q_x and q_y, respectively; l is the spring length in axial direction. Let $p = i\omega$, then from $D(i\omega, q_x, q_y) = 0$ find relation of frequency ω and q_x, q_y:

$$\omega^{\pm} = \sqrt{\left(\frac{a_{11} + a_{22}}{2} \pm \sqrt{\frac{(a_{11} - a_{22})^2}{4} + a_{12}^2}\right)\frac{1}{M}}. \tag{4}$$

Phase velocity vector and its modulus are determined with the formulas:

$$\vec{c}_f^{\pm} = \frac{\omega^{\pm}}{q_x^2 + q_y^2}(q_x, q_y), \quad \left|\vec{c}_f^{\pm}\right| = \frac{\omega^{\pm}}{\sqrt{q_x^2 + q_y^2}}. \tag{5}$$

The group velocity vector and its modulus are:

$$\vec{c}_g^{\pm} = \left(\frac{\partial\omega^{\pm}}{\partial q_x}, \frac{\partial\omega^{\pm}}{\partial q_y}\right), \quad \left|\vec{c}_g^{\pm}\right| = \sqrt{\left(\frac{\partial\omega^{\pm}}{\partial q_x}\right)^2 + \left(\frac{\partial\omega^{\pm}}{\partial q_y}\right)^2}. \tag{6}$$

So, each couple of wave numbers q_x, q_y corresponds to two waves with propagation velocities c_f^+ and c_f^- and frequencies ω^+ and ω^-.

It follows from (4), (5):

$$\omega^{\pm}\Big|_{q_x = q_y = \pi/l} = 2\sqrt{\frac{k_1}{M}} = \omega_0, \quad \omega^{\pm}\Big|_{q_x = \pi/l,\, q_y = 0} = \omega^{\pm}\Big|_{q_x = 0,\, q_y = \pi/l} = \sqrt{\frac{2}{M}(2k_2 + k_1 \pm k_1)} = \omega_1^{\pm}; \tag{7}$$

$$\left|\vec{c}_f^{\pm}\right|_{q_x = q_y = \pi/l} = \frac{l}{\pi}\sqrt{\frac{2k_1}{M}} = \frac{l\omega_0}{\pi\sqrt{2}} = c_0, \quad \left|\vec{c}_f^{\pm}\right|_{q_x = \pi/l,\, q_y = 0} = \left|\vec{c}_f^{\pm}\right|_{q_x = 0,\, q_y = \pi/l} = \frac{l\omega_1^{\pm}}{\pi} = c_1^{\pm}. \tag{8}$$

As is evident, the solutions for frequencies and phase velocities coincide at the point $q_x = q_y = \pi/l$. As $q_x, q_y \to 0$, we have that $\omega \to 0$. When $q_x, q_y \to 0$, the values of the moduli of phase and group velocities have different limits depending on ratio of q_x and q_y. If $q_x = 0$ and $q_y \to 0$, or $q_x \to 0$ and $q_y = 0$, then:

$$\left|\vec{c}_f^{\pm}\right| = \left|\vec{c}_g^{\pm}\right| = l\sqrt{\frac{2k_2 + k_1 \pm k_1}{2M}} = \frac{l\omega_1^{\pm}}{2} = c_2^{\pm}. \tag{9}$$

If $q_x = q_y = q$ and $q \to 0$, then:

$$\left|\vec{c}_f^{\pm}\right| = \left|\vec{c}_g^{\pm}\right| = l\sqrt{\frac{k_1 + 2k_2 \pm 2k_2}{2M}} = c_3^{\pm}. \tag{10}$$

The group velocity moduli $\left|\vec{c}_g^{\pm}\right|$ at the points $U(q_x = q_y = \pi/l)$, $X(q_x = \pi/l, q_y = 0;$ $q_x = 0,\ q_y = \pi/l)$ equal zero. Also, when $k_1 \le 4k_2$, then at the point $K(q_x = q_y = \arccos(-k_1/4k_2)/l)$ we have that $\vec{c}_g^{+} = 0$. Consequently, according to [20], frequencies ω_0, $\omega_1^{\pm}$, ω_2^{+} are resonant for this system and:

$$\omega_2^{+} = \omega_K^{+} = 2(1 + k_1/4k_2)\sqrt{k_2/M}. \tag{11}$$

It follows from the comparison of (9) and (10) that the long wave velocity is the same in the diagonal and axial directions if $k_1 = 2k_2$. Figure 2 illustrates relationship of the phase velocity frequency and modulus and the wave numbers q_x, q_y for $k_1 = 2k_2 = 4/3$. Hereinafter, it is assumed that the masses of balls and lengths of springs are: $M = 1$, $l = 1$. The choice of k_1 and k_2 was based on the condition that $k_1 + k_2 = 2$. The velocity unit was accepted $c = l\sqrt{k/M}$, where $k = 1$.

For $k_1 = 2k_2 = 4/3$, when the long wave velocities along the axes and diagonals are equal, and for $k_1 = 0.2$, $k_2 = 1.8$ and $k_1 = 1.8$, $k_2 = 0.2$, the wave frequencies in the lattice against the modulus of the wave vector at the boundaries of a triangle in the plane (q_x, q_y) with corners at the points $\Gamma(q_x = q_y = 0)$, U and X are shown in Fig. 3 in the form of Brillouin's diagrams [16]. It is seen that the range of allowed frequencies is, according to (7): $0 \le \omega \le \omega_1^{+}$. When the frequencies are low, the curves approach straight lines with inclines to the axis of wave vectors depending on the ratio of the stiffnesses k_1 and k_2. According to (9), (10), these inclines determine the values of the phase and group velocities. For instance, the circled extremums in Fig. 3 fit with the above-determined resonant frequencies ω_0, $\omega_1^{\pm}$, ω_2^{+}.

Analysis of the surface of the phase velocity moduli for the two waves and for $k_1 = 0.2$, $k_2 = 1.8$ in Fig. 4*a* as well as for $k_1 = 1.8$, $k_2 = 0.2$ in Fig. 4*b* shows that if $k_1 \ne 2k_2$, velocity of long waves ($\sqrt{q_x^2 + q_y^2} < \varepsilon$, ε is low) greatly depends on the wave direction. For example, it follows from Fig. 4*a* that the maximum velocity features the waves c_f^{+} running along the diagonals, while in Fig. 4*b* the axial waves have the velocity maxima. The situation is opposite for the waves c_f^{-} though the maximal velocities are lower than in c_f^{+}. The phase and group velocities of the both waves coincide in the lower frequency spectrum. Therefore the long waves propagate without dispersion and generate quasi-front [19] of a low-frequency pendulum wave.

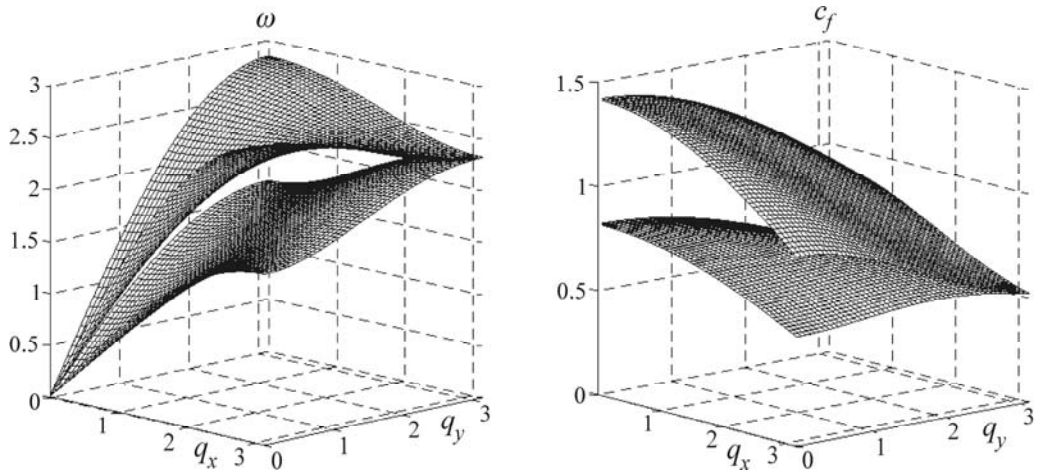

Fig. 2. Relationship of the frequency and modulus of phase velocity and the wave numbers q_x, q_y ($k_1 = 2k_2 = 4/3$)

The equations (3) in a continuum agree with the equations of the orthotropic elasticity theory. Assume that $l \to 0$ and obtain:

$$M\ddot{u}_{n,m} = l^2\left[(k_1 + k_2)\frac{\partial^2 u}{\partial x^2} + k_2\frac{\partial^2 u}{\partial y^2} + 2k_2\frac{\partial^2 v}{\partial x \partial y}\right] + Q_x,$$

$$M\ddot{v}_{n,m} = l^2\left[k_2\frac{\partial^2 v}{\partial x^2} + (k_1 + k_2)\frac{\partial^2 v}{\partial y^2} + 2k_2\frac{\partial^2 u}{\partial x \partial y}\right] + Q_y.$$

If $k_1 = 2k_2$, these equations describe plane deformation of an isotropic elastic medium with a Poisson ratio. This conclusion accords with the earlier outcome that when $k_1 = 2k_2$ the long waves have equal velocities in any directions (refer to Fig. 2).

To study an unsteady wave process, assume that a lattice is infinite and forces are applied at the points with the coordinates:

$$(n_0 - 1, m_0 - 1), (n_0 - 1, m_0), (n_0, m_0 - 1), (n_0, m_0)$$

as shown in Fig. 5. The equations (3) are solved with using the finite difference method.

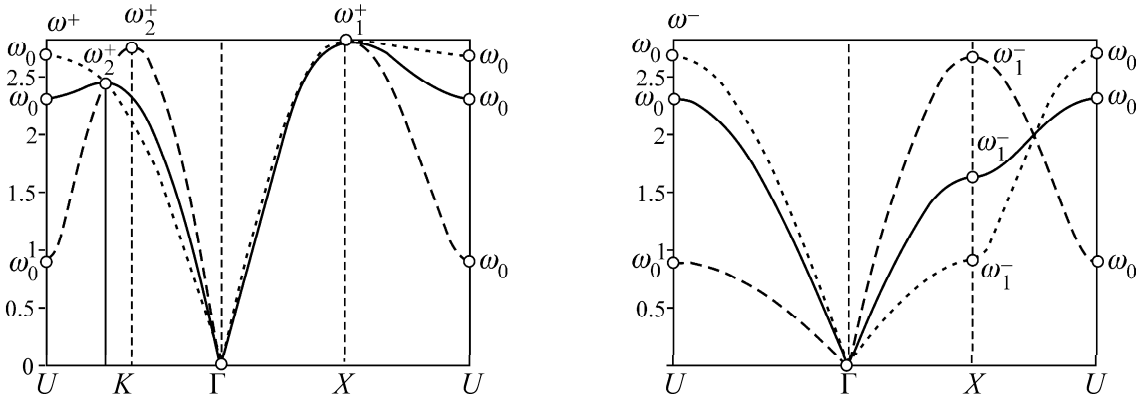

Fig. 3. The Brillouin diagram for the lattice in Fig. 1: the wave frequencies against the wave vector modulus along the boundaries of the triangle $\Gamma(q_x = q_y = 0)$, $U(q_x = q_y = \pi/l)$, $X(q_x = \pi/l, q_y = 0)$ in the plane (q_x, q_y). The solid curves show $k_1 = 2k_2 = 4/3$, dotted curves are for $k_1 = 1.8$, $k_2 = 0.2$, and the dashed curves are for $k_1 = 0.2$, $k_2 = 1.8$

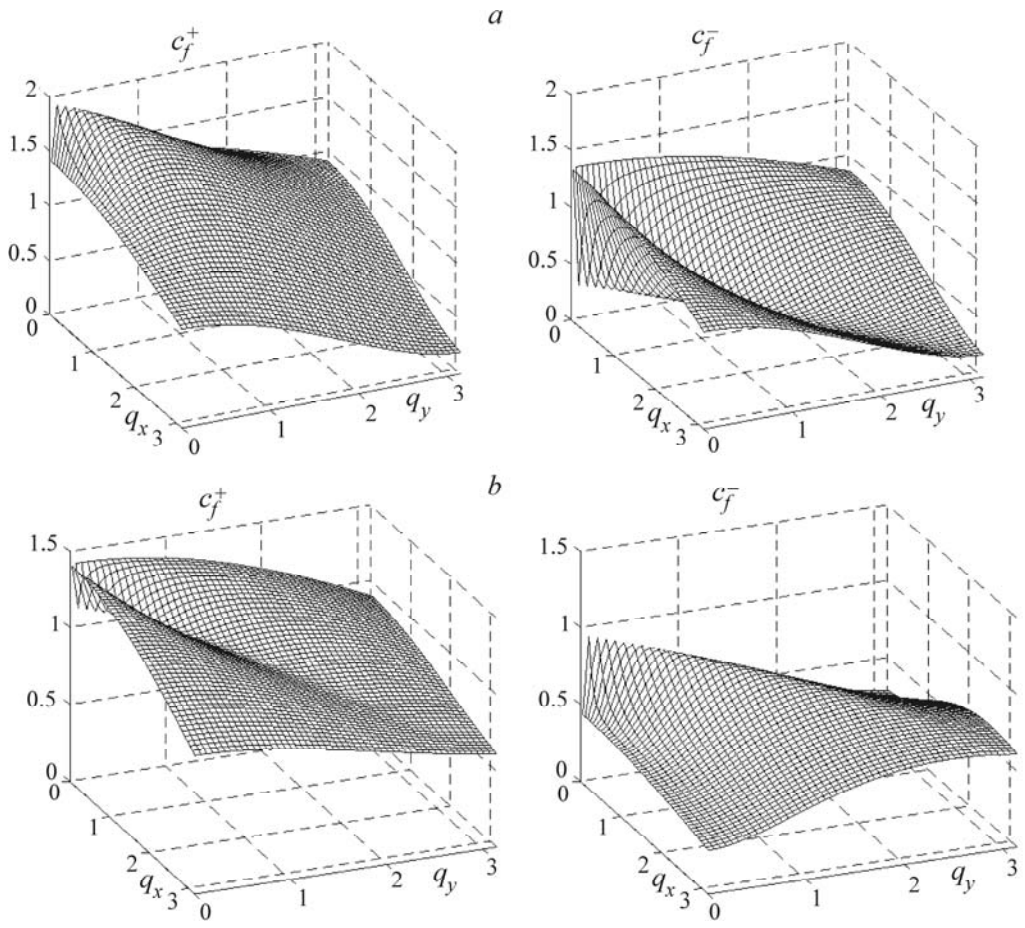

Fig. 4. The phase velocity modulus versus the wave numbers q_x, q_y: *a* — $k_1 = 0.2$, $k_2 = 1.8$; *b* — $k_1 = 1.8$, $k_2 = 0.2$

Figure 6 presents calculation results for the radial displacement at the time $T = 36$:

$$u_r(n,m) = \frac{u_{n,m}(n - n_0 + a_n) + v_{n,m}(m - m_0 + a_m)}{\sqrt{(n - n_0 + a_n)^2 + (m - m_0 + a_m)^2}},$$

$$a_n = \begin{cases} 0 & \text{if} \quad n \ge n_0 \\ 1 & \text{if} \quad n < n_0 \end{cases}, \quad a_m = \begin{cases} 0 & \text{if} \quad m \ge m_0 \\ 1 & \text{if} \quad m < m_0 \end{cases}$$

for the influence by stages: $Q(t) = Q_0 H_0(t)$, where $H_0(t)$ is the Heaviside function. The problem involved the parameters: $\tau = 0.07$, $n_0 = m_0 = 60$, where τ was the time step. The stiffness of the diagonal and axial springs was different: $k_1 = 0.2$, $k_2 = 1.8$ (see Fig. 6*a*); $k_1 = 2k_2 = 4/3$ (Fig. 6*b*); $k_1 = 1.8$, $k_2 = 0.2$ (Fig. 6*c*).

It is seen in Fig. 6*a* that when $k_1 < 2k_2$, the axial long waves have lower velocity as against the diagonal long waves. Vice versa, if $k_1 > 2k_2$, the axial velocities are higher than the diagonal velocities as is in Fig. 6*c*. In the case of $k_1 = 2k_2$, the lattice is "isotropic": the waves go as circles (Fig. 6*b*). The conclusions agree in full with the phase surfaces in Figs. 2 and 4.

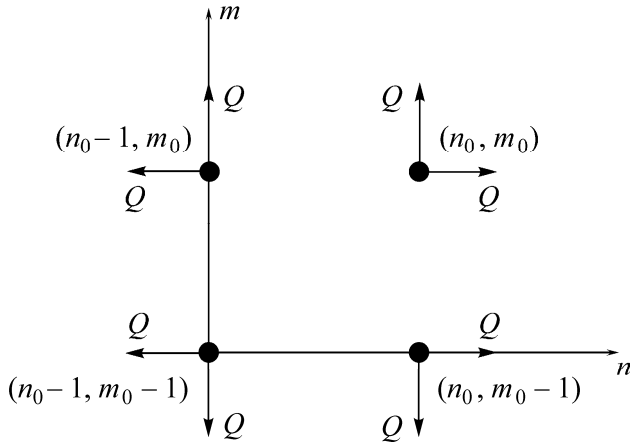

Fig. 5. Scheme of point sources

We model the impact with frequency ω_* as follows:

$$Q(t) = H_0(t)H_0(\pi - \omega_* t)\sin\omega_* t\,.$$

Figures $7-9$ show oscillograms of the radial velocity $\dot{u}_r(n,m)$ at the axial point $n = n_0$, $m - m_0 = 20$ and at the diagonal point $n - n_0 = m - m_0 = 20$, as well as their spectral density $G(\omega, n, m) = \left| \int_0^T \dot{u}_r(n,m)e^{-i\omega t}\,dt \right|$, which was calculated with the fast Fourier transform. The problem parameters were: $\tau = 0.07$, $\omega_* = 5$, $n_0 = m_0 = 430$; $T = 287$ in Figs. 7 and 8; $T = 574$ in Fig. 9. The stiffness of the springs was different: $k_1 = 0.2$, $k_2 = 1.8$ in Fig. 7; $k_1 = 2k_2 = 4/3$ in Fig. 8; $k_1 = 1.8$, $k_2 = 0.2$ in Fig. 9.

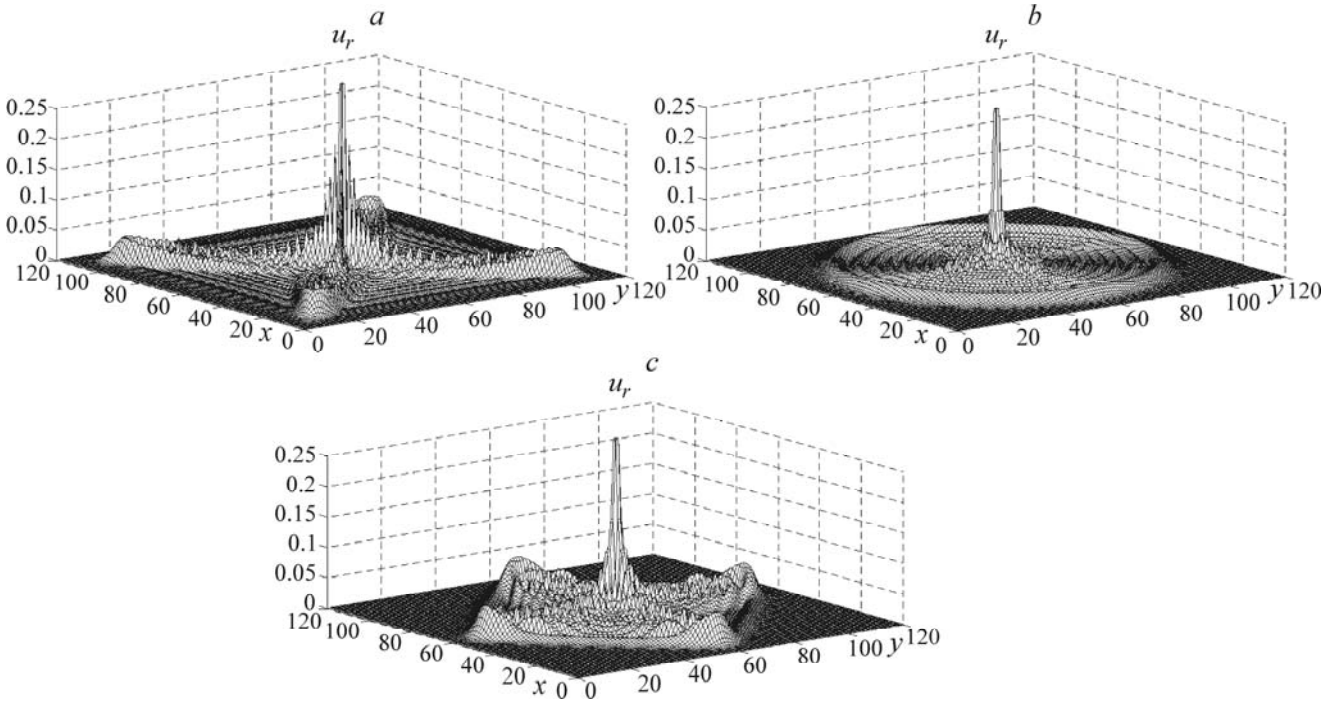

Fig. 6. Radial displacement: *a* — $k_1 = 0.2$, $k_2 = 1.8$; *b* — $k_1 = 2k_2 = 4/3$; *c* — $k_1 = 1.8$, $k_2 = 0.2$

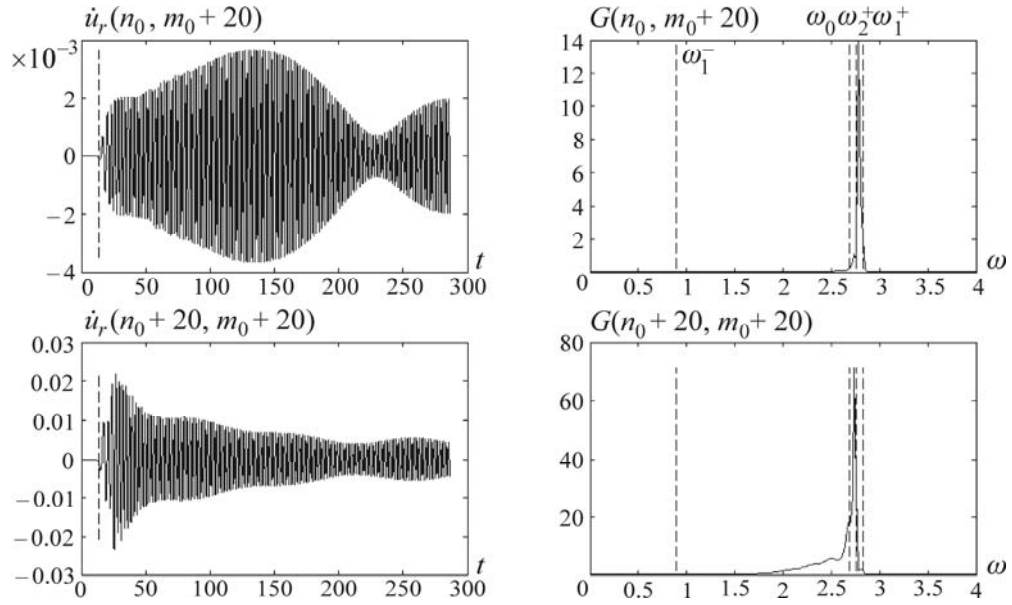

Fig. 7. Radial velocity and its spectrum for $k_1 = 0.2$, $k_2 = 1.8$

Vertical lines in the oscillograms show arrival times of the long waves with the velocities c_f^+. At the axial points ($n = n_0$ or $m = m_0$), the arriving waves have the velocity $c_2^+ = l\sqrt{(k_1 + k_2)/M}$ at $t = (m - m_0)l/c_2^+$. At the diagonal points ($n - n_0 = m - m_0$), the arriving waves have $c_3^+ = l\sqrt{(k_1 + 4k_2)/2M}$ at $t = (m - m_0)l\sqrt{2}/c_3^+$. As is seen in Figs. 8 and 9, the arrivals of the long waves at the specified points are calculated, to within a small percentage, by (9), (10). The waves, which have "+" in Eqs. (4) – (10), are the analog of longitudinal disturbances in elastic bodies, and the waves with "–" are analogous to shear waves. The short "longitudinal" waves have lower velocity than the long waves. By the analysis of the numerical results, in the lattice with two directions of links (diagonal and axial), there are two directions of short waves: diagonal and axial. The same situation was revealed in the antiplane plane problem on the local periodical loading of a lattice with a resonant frequency (waves propagated in the diagonal direction only) [20]. These are the so called "star waves". Depending on the ratio of the stiffnesses k_1, k_2, the "star waves" run either diagonal only (Fig. 6*a*), or axially (Fig. 6*c*), or in the diagonal and axial directions, both (Fig. 6*b*).

As per the analysis of the oscillograms, the axial velocities have the order lower amplitudes as against the diagonal velocities if $k_1 < 2k_2$. If the spring stiffness in the axial direction is twofold the diagonal spring stiffness, then the axial waves have much higher amplitudes as compared with the diagonal disturbance.

In the spectral density plots (Figs. 7 – 9), the vertical lines show the resonant frequencies ω_0, $\omega_1^\pm$, ω_2^+ from (7), (11). This axially symmetrical impulsive impact, as it follows from Figs. 7 – 9, excites mainly oscillations with ω_1^+ and ω_2^+. This is in accord with the "expansion" waves with the length $\lambda = 2l$ and $\lambda = 2l\pi/\arccos(-k_1/4k_2)$.

Figure 10 displays oscillograms of radial velocities at various distances from the impact. The problem parameters are identical to the parameters of the problem in Fig. 9. It is seen in Fig. 10 that the wave amplitudes get lower with the distance from the impact.

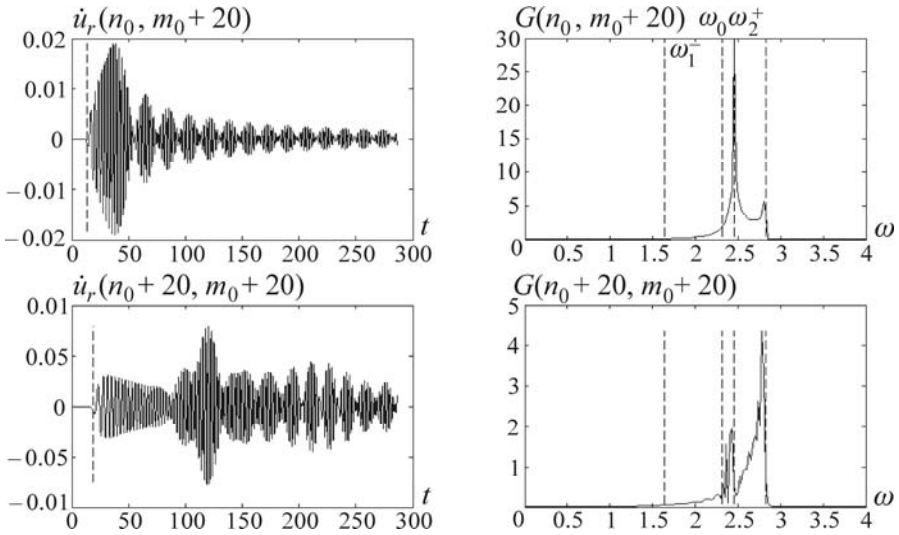

Fig. 8. Radial velocity and its spectrum for $k_1 = 2k_2 = 4/3$

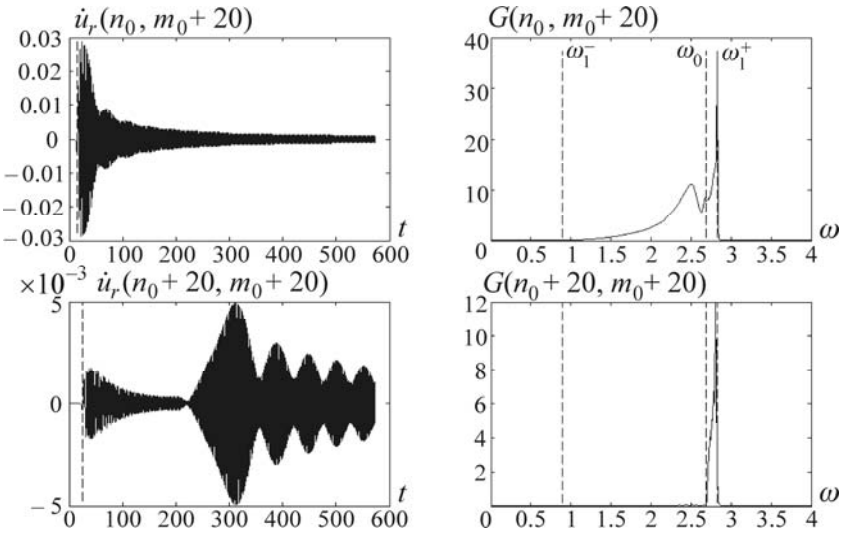

Fig. 9. Radial velocity and its spectrum for $k_1 = 1.8$, $k_2 = 0.2$

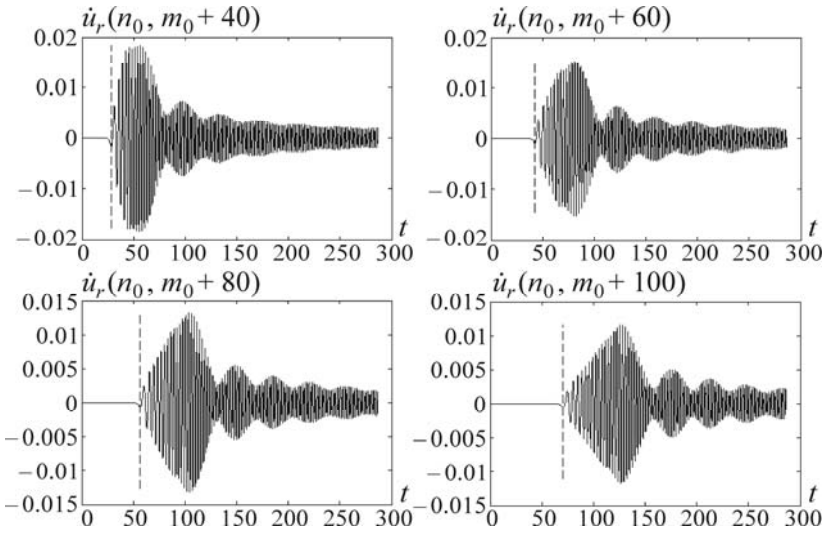

Fig. 10. Radial velocity for $k_1 = 1.8$, $k_2 = 0.2$

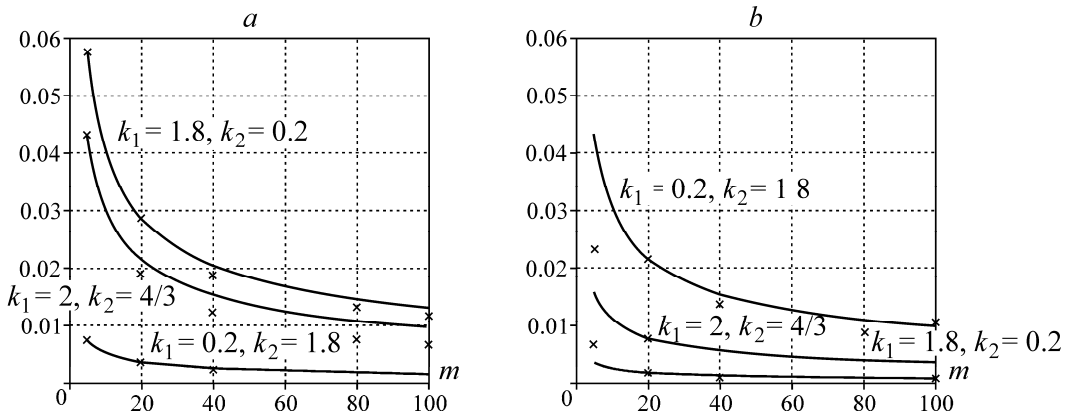

Fig. 11. Maximal radial velocities of masses depending on the distance to the point source: *a* — in the line of axis; *b* — in the diagonal

See Fig. 11 with graphs of the maximal amplitudes of the travel velocities depending on the distance to the impact point. Criss-crosses show the numerical results. The problem parameters are the same as in Figs. 7 – 9. The solid curves show functions that are proportional to $1/\sqrt{m - m_0}$ and coincide with the calculated maxima of the velocity amplitudes at the distance of 5 lattice steps from the point source for the case when the impact is on the axis and at the distance of 20 lattice steps for the case when the impact is on the diagonal. It is seen that the qualitative behavior of the wave amplitude versus distance curve is well described by the mentioned function, which is characteristic to cylindrical waves in an elastic medium under impulsive point source effect.

CONCLUSION

The simulation of the dynamic behavior of a block-structured medium has shown that the existence of the structure changes the medium behavior. Taking account of the structure limits, the frequency spectrum of waves in the block-structured medium characterized by spatial anisotropy. The difference from a continuous medium is especially acute under impulse loading when the load application time is shorter than the period of all waves in the block-structured medium.

The two-dimension model calculations have shown that in the block-structured medium exposed to impulse loading:

- Spectrum of the disturbance depends on the resonant frequencies of the medium;
- Velocity of the low frequency pendulum waves varies in different directions;
- In the square lattice model of flat motion in the block-structured medium, waves propagate generally in the direction along which the stiffness of the links is maximal;
- Behind the low frequency waves in the axial and diagonal directions, a short wave "tail" originates; frequency of these short waves is close to resonant frequencies but amplitude is much higher than is typical to low frequency waves. These short waves are the so called "star waves".

The study was conducted with financial support from the Russian Foundation for Basic Research, Project No. 08-05-00509, and from the Siberian Branch, Russian Academy of Sciences, Integration Project No. 74.

REFERENCES

1. M. A. Sadovsky, "Natural lumpiness of rocks," *Dokl. Akad. Nauk SSSR*, **247**, No. 4 (1979).
2. M. V. Kurlenya, V. V. Adushkin, and V. N. Oparin, "Alternating response of rocks to the dynamic impact," *Dokl. Akad. Nauk SSSR*, **323**, No. 2 (1992).

3. M. V. Kurlenya, V. N. Oparin, P. F. Morozov, et al., "Phenomenon of self-organization in artificial masses with the formation of cellular structure consisted of cells with a passive core and active shell," *Dokl. Akad. Nauk SSSR*, **323**, No. 6 (1992).
4. M. V. Kurlenya, V. N. Oparin, and V. I. Vostrikov, "Formation of elastic wave packages in the block-structured medium under impulse loading. Pendulum type waves," *Dokl. Akad. Nauk SSSR*, **333**, No. 4 (1993).
5. M. V. Kurlenya, V. N. Oparin, and V. I. Vostrikov, "Pendulum-type waves. Part II: Experimental methods and main results of physical modeling," *Journal of Mining Science*, No. 4 (1996).
6. M. V. Kurlenya, V. N. Oparin, V. I. Vostrikov, et al., "Pendulum-type waves. Part III: Data of on-site observations," *Journal of Mining Science*, No. 5 (1996).
7. N. I. Aleksandrova, "Elastic wave propagation in block medium under impulse loading," *Journal of Mining Science*, No. 6 (2003).
8. N. I. Aleksandrova and E. N. Sher, "Modeling of wave propagation in block media," *Journal of Mining Science*, No. 6 (2004).
9. N. I. Aleksandrova, A. G. Chernikov, and E. N. Sher, "Experimental investigation into the one-dimensional calculated model of wave propagation in block medium," *Journal of Mining Science*, No. 3 (2005).
10. E. N. Sher, N. I. Aleksandrova, M. V. Ayzenberg-Stepanenko, and A. G. Chernikov, "Influence of the block-hierarchical structure of rocks on the peculiarities of seismic wave propagation," *Journal of Mining Science*, No. 6 (2007).
11. N. I. Aleksandrova, E. N. Sher, and A. G. Chernikov, "Effect of viscosity of partings in block-hierarchical media on propagation of low-frequency pendulum waves," *Journal of Mining Science*, No. 3 (2008).
12. V. A. Saraikin, "Calculation of wave propagation in the two-dimensional assembly of rectangular blocks," *Journal of Mining Science*, No. 4 (2008).
13. V. A. Saraikin, "Elastic properties of blocks in the low-frequency component of waves in a 2D medium," *Journal of Mining Science*, No. 3 (2009).
14. V. A. Saraikin, "Low-frequency wave propagation in a block structured model," *Prikl. Mekh. Tekh. Fiz.*, No. 6 (2009).
15. C. Lord Rayleigh, "On the maintenance of vibrations by forces of double frequency, and the propagation of waves through a medium endowed with periodic structure," *Phil. Mag*., **145** (1887).
16. L. Brillouin, *Wave Propagation in Periodic Structures*, Dover Publication, New York (1953).
17. A. A. Maradudin, E. W. Montroll, and G. H. Weiss, *Theory of Lattice Dynamics in the Harmonic Approximation*, Academic Press, New York (1963).
18. D. J. Mead, "Vibration response and wave propagation in periodic structures," *J. Eng. in Industry*, **93** (1971).
19. L. I. Slepyan, *Nonstationary Elastic Waves* [in Russian], Sudostroenie, Leningrad (1972).
20. M. Ayzenberg-Stepanenko and L. Slepyan, "Resonant-frequency primitive waveforms and star waves in lattices," *Journal of Sound and Vibration*, **313** (2008).
21. N. I. Aleksandrova, M. V. Ayzenberg-Stepanenko, and E. N. Sher, "Modeling the elastic wave propagation in a block medium under the impulse loading," *Journal of Mining Science*, No. 5 (2009).
22. J. S. Jensen, "Phononic band gaps and vibrations in one- and two-dimensional mass – spring structures," *Journal of Sound and Vibration*, **266** (2003).